Measuring Ligand−Receptor Unbinding Forces with Magnetic Beads: Molecular Leverage†

Z. Guttenberg,‡ A. R. Bausch,‡ Bin Hu,‡ R. Bruinsma,§ L. Moroder,|| and E. Sackmann*,‡

Department of Physics, University of California, Los Angeles, California 900024, MPI for Biochemistry, Am Klopferspitz 18a, 82152 Martinsried, Germany, and Physik Department E22, Technische Universität München, James-Franck-Strasse 1, D-85748 Garching, Germany

Received February 28, 2000. In Final Form: May 25, 2000

We describe a new method for the quantitative measurement of weak forces between adhesion domains formed by receptor−ligand pairs. The method relies on the microinterferometric analysis of adhering vesicles subjected to an external force produced by a magnetic bead adhered to the membrane. The forces exerted on pinning centers can be deduced using classical elasticity theory. The method is applied to measure the binding strengths between solubilized solid supported integrin receptors $\alpha_{IIb}\beta_3$ of blood platelets and lipid-coupled cyclic peptides containing arginine−glycine−aspartate (RGD) tripetide ligands, embedded in the vesicle, that are recognized selectively by the integrins. We find that unbinding takes place at force levels far below those found in single-molecule studies. We interpret our findings in terms of the fracturing of the receptor−ligand pairs by the torque generated by the force which is much more effective than the traction.

I. Introduction

Recognition between cells is based on the interaction between membrane-bound receptor proteins with specific ligands embedded in the partner membrane. The equilibrium binding free-energy of ligand−receptor pairs can be obtained by classical thermodynamic methods. Measurement of the forces exerted between partner membranes during bioadhesion is a more difficult problem. One the one hand, macroscopic methods, such as the force apparatus,[1] allow delicate measurement of bioadhesion forces between receptor/ligand partner membranes, provided the membranes remain homogeneous. However, it has become evident, from microscopy studies on model systems and from in vivo studies, that bioadhesion generically leads to decomposition phenomena: the formation of ligand/receptor pairs, known as "focal adhesion sites" (FAS), is observed producing highly heterogeneous adhesion disks. Macroscopic methods are less informative under these conditions. On the other hand, the recent development of nanoprobe techniques now allow direct measurement, at the single-molecule level, of the forces required to unbind macromolecule ligand−receptor pairs.[2,3] The results obtained by these methods show (i) that the ligand/receptor unbinding force must be considered as a a statistical quantity and (ii) that the unbinding force depends strongly on the *ramping rate* at which the force is applied, thus proving evidence for the so-called Bell model of adhesion.[4] The statistical nature of ligand−receptor rupture during cell adhesion was also clearly demonstrated by flow chamber experiments[5,6] and Dustin[7] provided strong evidence that the receptor−ligand bond formation is reversible and may thus be described in terms of a model for thermodynamic equilibrium. Depending on the ramp rate, the ligand/receptor unbinding force can vary from a few piconewtons to hundreds of piconewtons.[2,3]

It is important to note though that for a number of reasons the interaction between receptors and conjugate ligands in biology is not really a "single-molecule" property: (i) the adhesion proteins are embedded in a soft body (the cell membrane) that is known to deform very considerably indeed under the point forces generated by the nanoprobe techniques; (ii) membrane-bound "repeller" molecules—such as glycoproteins and oligosaccharides—reduce the adhesion free energy and promote formation of focal adhesion sites,[8] and (iii) bonded pairs of adhesion molecules are likely to be in local chemical equilibrium with free ligands and receptors. It has been shown both theoretically and experimentally that this "collective" effect results in a significant lowering of the effective adhesion free energy.[8]

In this paper we report on a "mesoscopic" method for measuring ligand−receptor forces that aims at avoiding the drawbacks of both the macroscopic and the single-molecule methods. Lift forces—in the 0.1 to 2 pN range—are generated on adherent membranes by pulling on the adhering vesicle in the normal direction with a magnetic bead attached to the top of the adherent vesicle. The heterogeneous structure of the adhesion disk—as well as the unbinding of various FAS—are then monitored by reflection interference contrast microscopy (RICM). Both the magnitude and the direction of the forces exerted on individual adhesion sites can be determined *quantitatively*, from the RICM patterns by applying methods borrowed

† Part of the Special Issue "Colloid Science Matured, Four Colloid Scientists Turn 60 at the Millennium".

* To whom correspondence may be addressed.
‡ Technische Universität München.
§ University of California.
|| MPI for Biochemistry.

(1) Israelachvili, J. N. *Intermolecular and Surface Forces*, 2nd ed.; Academic Press: London, 1991.
(2) Merkel, R.; Nassoy, P.; Leung, A.; Ritchie, K.; Evans, E. *Nature* **1999**, *397*, 50−53.
(3) Simson, D. A.; Strigl, M.; Hohenadl, M.; Merkel, R. *Phys. Rev. Lett.* **1999**, *83*, 652−655.
(4) Bell, G. I. *Science* **1978**, *200*, 618−627.
(5) Kaplanski, G.; Farnarier, C.; Tissot, O.; Pierres, A.; Benoliel, A. M.; Alessi, M. C.; Kaplanski, S.; Bongrand, P. *Biophys. J.* **1993**, *64*, 1922−33.
(6) Alon, R.; Hammer, D. A.; Springer, T. A. *Nature* **1995**, *377*, 86.
(7) Dustin, M. L. *J. Biol. Chem.* **1997**, *272*, 15782−15788.
(8) Bruinsma, R.; Behrisch, A.; Sackmann, E. *Phys. Rev. E*, in press.

10.1021/la000279x CCC: $19.00
Published on Web 07/28/2000

from the classical theory of elasticity[9] applied to soft shells (cf. refs 8 and 10). The unbinding force of an individual FAS may be determined in this manner.

To test the technique, we measured the binding strength of focal adhesion sites formed by the integrin receptor $\alpha_{IIb}\beta_3$ of blood platelets paired with lipid coupled artificial ligands: cyclic peptides containing arginine−glycine−aspartic acid sequences ("RGD" sequences).[11] The cyclic peptides were reconstituted into giant vesicles—acting as "test cells"—to form freely mobile ligands, while the integrins were attached to a solid support, thereby allowing application of the RICM technique. Mobile repeller molecules were embedded in the vesicle as well to make the system more realistic and to avoid nonspecific binding.

Depending on the integrin area concentration, our method indicates that *a FAS can unbind at sub-piconewton force levels*. This is a surprising result since for similar ramping rates, the nanoprobe techniques report higher unbinding forces *for individual receptor−ligand pairs*. The present work describes a new strategy to probe the forces between receptor ligand pairs under biologically relevant conditions and points out for the first time the important role of torques for fracturing of ligand receptor bonds in membranes. It is presently restricted to model membranes but it can be also applied to cells. A necessary albeit complicated next step is a more quantitative characterization of the receptor and ligand density and the development of techniques to control the density and mobility of surface and anchored receptors.

II. Materials and Methods

(A) Preparation and Force Calibration. Giant vesicles were prepared from a 1:1 mixture of dimyristoylphosphatidylcholine (DMPC) and cholesterol to which 1 mol % of PEG−lipopolymer (dimyristoylphosphatidylethanolamine with a poly(ethylene glycol) (PEG) headgroup of molecular weight 2000 purchased from Polar Lipids, Alabaster, AL) was added (the purity was >99%). These PEG−lipopolymers act as repellers and help to suppress nonspecific van der Waals adhesion. Moreover they promote formation of unilamellar vesicles. We also added 0.5 mol % of lipid-coupled cyclic hexapeptide containing a RGD sequence (Figure 1d) that is selectively recognized by the integrin $\alpha_{IIb}\beta_3$ receptor of blood platelets (ref 11 and unpublished results of the authors' laboratory). These ligands were synthesized in one of the authors laboratories (L.M.). Separate studies in the Munich laboratory show that the binding constant is $K_D \approx 1.1\ \mu$M, compared to the $K_D \approx 0.1\ \mu$M of the natural ligand fibrinogen.[12] Integrin receptors were prepared from blood platelets, solubilized by Triton X100, and fixed on a glass substrate by physisorption during incubation. For this purpose the Triton-solubilized integrin receptor was dissolved in Tris-buffer (20 mM Tris pH 7.25, 150 mM NaCl, 1 mM $MgCl_2$, 1 mM $CaCl_2$, 1 mM NaN_3, 0.01% Triton X100) and the substrates were incubated in this solution for 1 h. In a second step the substrates were incubated in a solution of 3 wt % bovine serum albumin (BSA) in HEPES buffer (10 mM HEPES pH 7.25, 100 mM NaCl, 1 mM $CaCl_2$, 1 mM NaN_3). After each incubation the substrates were thoroughly washed with HEPES buffer. We assume that residual Triton is removed during this procedure since no appreciable shape changes or instabilities of the giant vesicles were observed.

The giant vesicles were prepared by swelling under an ac electric field following ref 13. The lipid mixture was therefore deposited onto glass slides covered by indium−tin oxide by solvent evaporation, and swelling occurred by addition of 170 mM sucrose solution during 2 h under 10 Hz and 1 V amplitude. Since the molar fractions of PEG lipopolymers and lipid-coupled RGD ligands added to the chloroform solution of the lipids were around 1%, it is reasonable to assume that the components are completely reconstituted in the vesicles. The efficiency of the reconstitution was further checked by differential calorimetry. We found broadening of the main transition peak with increasing RGD−lipid concentration up to 7 mol %, which provides further evidence for the above conclusion. Due to the presence of the PEG−lipid, most vesicles were unilamellar and the giant vesicles were stable for several hours.

By adjusting the receptor concentration in the buffer, we could control the receptor area density on the substrate. Nonspecific binding was suppressed not only by reconstitution of PEG−lipids but also by coating the substrate with BSA. As a result, no appreciable adhesion was observed either in the absence of grafted integrins or after photochemical denaturation of the receptor.

To couple the—highly monodisperse—magnetic beads (M450 Dynabeads, Dynal, Norway) to the vesicle, they were functionalized by anchoring solublized integrin receptors to the surface. For this purpose, the beads were first washed in borate buffer and then incubated in a solution of 0.4 mg/mL integrin and borate buffer for 24 h at 4 °C. The magnetic force exerted on a single magnetic bead by the magnetic field—produced by a solenoid with an hysteresis free soft iron core—was calibrated as follows. First, we measured the bead velocity in a viscous solution with a known viscosity (glycerol with 29 wt % $CsCl_2$) and used the Stokes formula to obtain the force exerted on the bead. Next, the force on magnetic beads attached to vesicles was calibrated by using them to lift spherical vesicles, filled with sucrose solution, against gravity. The minimum force required to lift the vesicle from the substrate was determined microscopically using RICM. Since the gravitational force is known, from the density difference between the inner and outer media, the force generated on the vesicle by the magnetic field could be determined. By a combination of these methods, we obtained the functional dependence between the bead force and the solenoid current. Typical force levels are in the range of 0.1−2 pN.

(B) Contour Force Analysis. To examine vesicle adhesion, and to analyze their contour near the substrate, the RICM method was applied, as described previously,[8,14] using a Zeiss Axiomat inverted microscope. As shown in Figure 1c, this method produces a set of equal-height contours of the vesicle in the vicinity of the adhesion area. In previous work we showed how the adhesion free energy of adhering vesicles in thermodynamic equilibrium can be obtained by measuring height contours near the adhesion disk. For a distance about 1 μm away from the contact line (the border of the adhesion disk), the vesicle surface is only weakly curved and a well-defined contact

(9) Landau, L. D.; Lifshitz, E. M. *Theory of Elasticity*; Pergamon Press: New York, 1986.
(10) Seifert, U.; Lipowsky, R. *Phys. Rev. A* **1990**, 4768−4771.
(11) Hu, B.; Baermann, M.; Sackmann, E. Submitted for publication in *Biochemistry*.
(12) Huber, W.; Hurst, J.; Schlatter, D.; Barner, R.; Huebscher, J.; Korns, W. G.; Steiner, B. *Eur. J. Biochem.* **1995**, *227*, 647−656.
(13) Dimitrov, D. S.; Angelova, M. I. *Bioelectrochem. Bioenerg.* **1998**, *253*, 323−336.
(14) Albersdoerfer, A.; Feder, T.; Sackmann, E. *Biophys. J.* **1997**, *73*, 245−257.

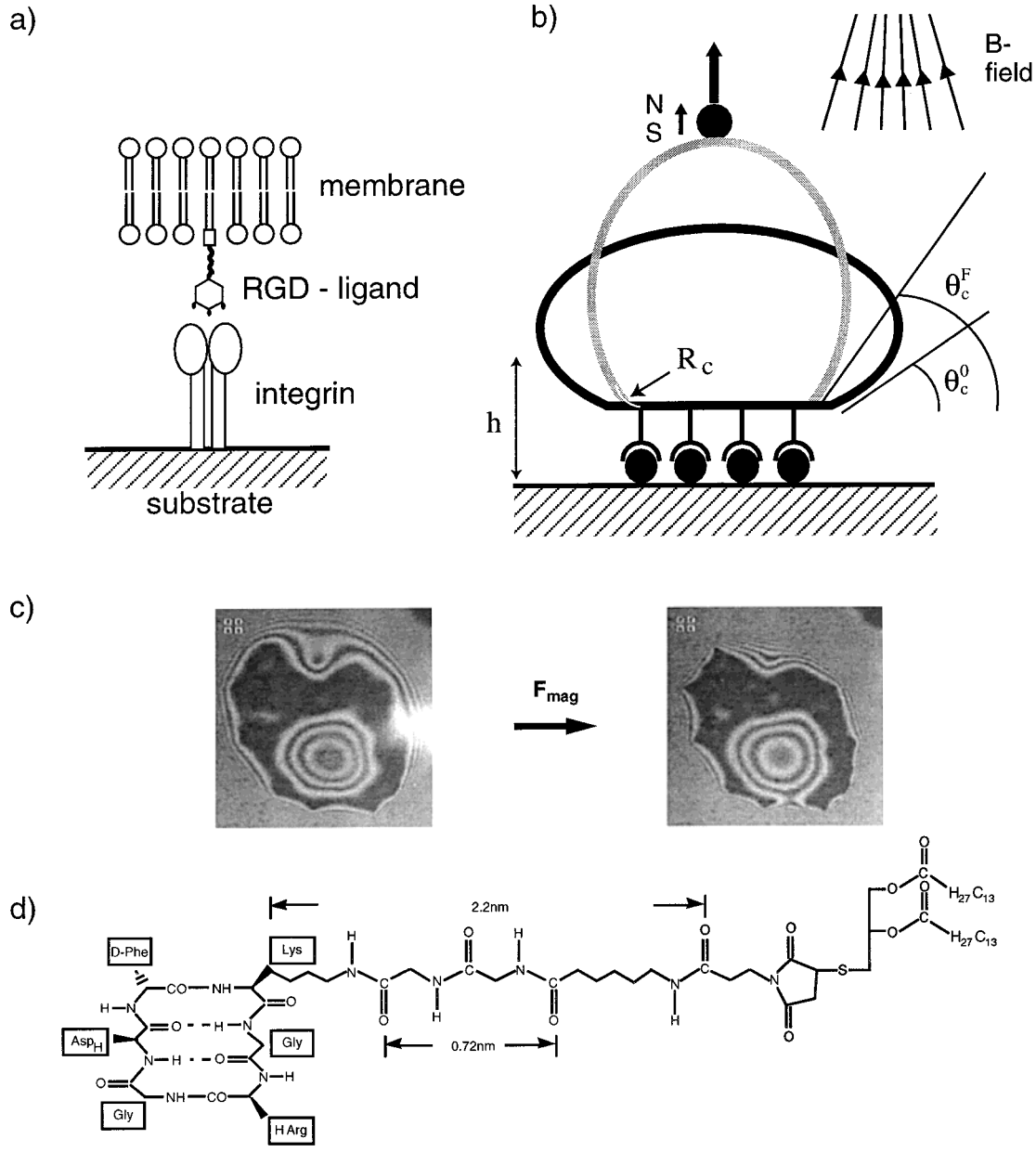

Figure 1. (a) Model system consisting of immobilized integrin receptors solubilized by surfactant (Triton X100) and lipid-coupled cyclic peptide containing an arginine−glycine−aspartate tripeptide sequence recognized by integrin receptors as selectively as natural ligands (e.g., fibrinogen). (b) Schematic view of force transducer consisting of a magnetic bead (acting as tweezers) which is coupled to the membrane at the top pole of vesicle and pulled in the vertical direction by inhomogeneous magnetic fields. (c) Example of giant vesicles adhering to substrate exhibiting clusters of immobilized integrin receptors. The black area defines the adhesion disk, and the array of Newtonian fringes in the center indicates a membrane blister bent toward the inside of the vesicle. By vertical deformation of the vesicle F_{mag} the pinning centers are exposed, exhibiting triangular shapes of the contact contour. (d) Chemical structure of the RGD lipopeptide, 0.5 mol % of this lipid was embedded into the giant vesicles.

angle θ can be found from the contours. This contact angle is related to the Gibbs adhesion free energy W and the vesicle tension γ by Young's law ($W = \gamma\ (1 - \cos\ \theta)$). A detailed study of the height contours near the contact line also reveals a highly curved section with a characteristic size given by the "capillary length" $\lambda = (\kappa/\gamma)^{1/2}$ with κ the Helfrich bending energy of the membrane and with γ the membrane tension. If the Helfrich bending energy is known, then the tension can be obtained by measuring λ (usually in the range of 0.1−1 μm (cf. Figure 2b for definition of λ from the height contours). Using Young's law then produces the Gibbs adhesion energy.

However, vesicles adhering to a substrate through mobile ligand−receptor pairs exhibit decomposition phenomena resulting in the formation of pinning sites that can contain large numbers of ligand−receptor pairs. As shown in Figures 1c and 2, these pinning sites show up as triangular cusps in the contact line if a force is applied on the upper pole of the vesicle. Note that the cusp angle decreases as we increase the force F exerted by the magnetic bead (cf. Figure 2a). The thermodynamic analysis mentioned above is, in general, not appropriate for such a heterogeneous adhesion disk in particular if the formation of pinning sites is irreversible (i.e., if thermal fluctuations are too weak to produce unbinding of pinning sites). It may still be possible, however, to determine the *forces* applied on a pinning site by the membrane from an analysis of the RICM contour profiles. The reason is that, under steady-state conditions, the nonadhering parts of the vesicle remain in local thermodynamic equilibrium

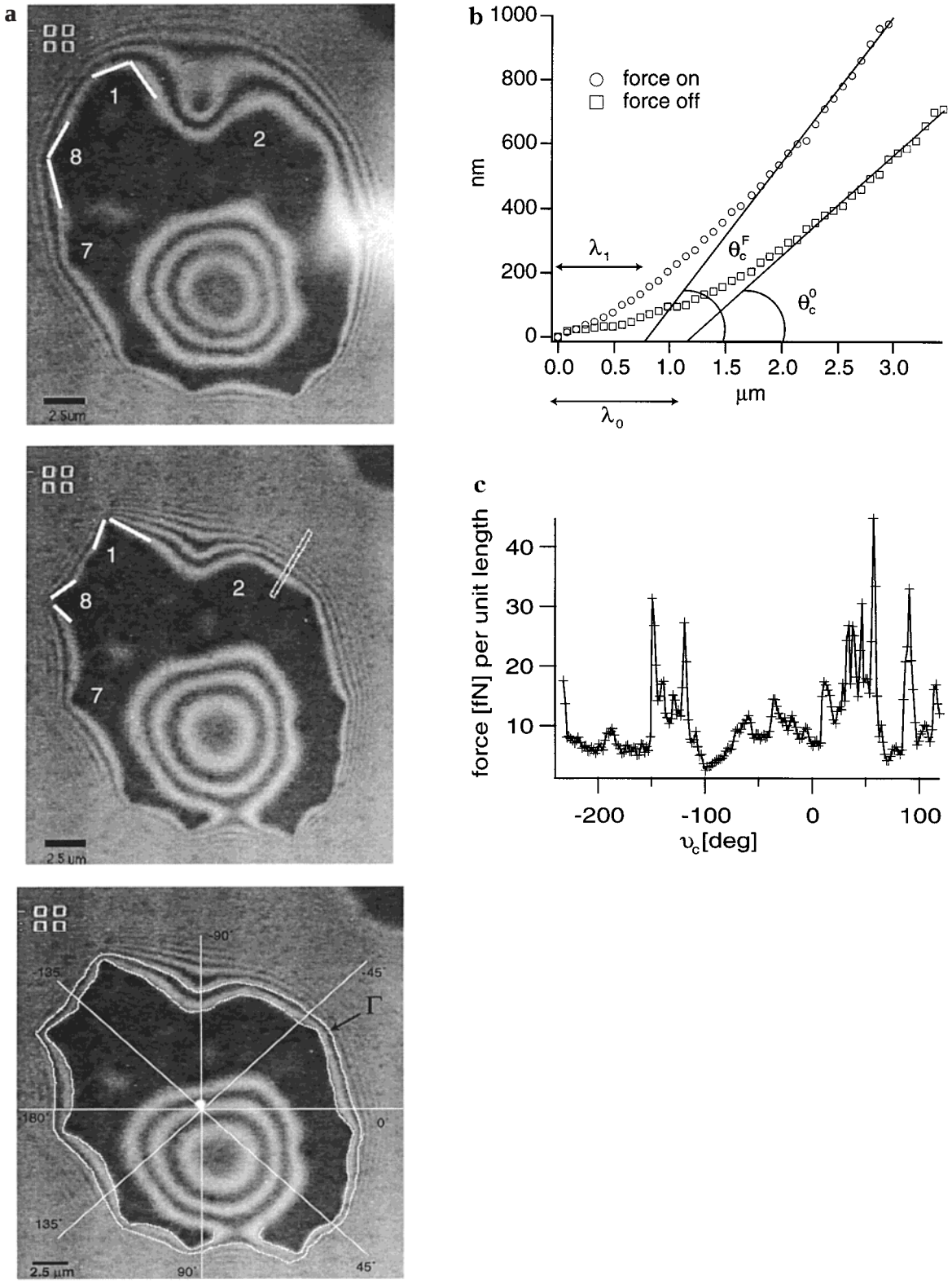

Figure 2. (a) RICM interferogram of vesicle in absence (top) and presence of 1.8 pN force (middle) showing the appearance of a pinning center after application of force. Note that the contact lines about the pinning centers exhibit triangular shapes and that the apex angel Φ decreases with force as indicated by the white angle in the top and middle image. The contour of the contact line and the first Newtonian fringe, respectively, are defined by white lines in the bottom image. (b) Contour of membrane along radial direction in area of weak adhesion (along the white bar of middle image of Figure 2a) in absence and presence of 1.8 pN external force. Note that contour consists of a curved region and a straight region. The slope of these straight line regions defines the contact angle θ_c. (c) Evalutaion of local force per unit length according to eq 3.

and can be described by the classical elastic free energy of a membrane (i.e., the sum of a bending energy part and a tension part). If this is the case, then by analyzing the shape of the nonadhering part of the membrane, we may deduce the forces and torques exerted by the membrane on a pinning site.

To see how, suppose that we determine the location of an equal height contour Γ some distance outside the

adhesion disk (i.e., at a distance exceeding λ) so we can neglect the curvature energy. The elastic free energy is then dominated by the tension γ. For the experiments described below, γ is the sum of a contribution due to the magnetic bead equal to $F/\pi D$, with F the vertical force exerted by the magnetic bead and D the maximum vesicle diameter plus an adhesion-induced tension γ_o (i.e., the tension for $F = 0$). Let $\tan \theta(s)$ be the slope of the vesicle surface perpendicular to the line of equal height (with s the arc length along the contour). $\theta(s)$ can be estimated—to a good approximation—by the distance $\Delta d(s)$ between the first and the second interference fringe (cf. Figure 2a bottom) at the point s according to

$$\theta(s) = \arctan(\Delta h/\Delta d(s)) \tag{1}$$

where Δh is the (fixed) height difference between interference fringes (equal to about $\lambda/4n = 102$ nm for $\lambda = 546$ nm and $n = 1.34$). The tension of the vesicle exerts a vertical force $f_\perp(s)$ per unit length on the contour line equal to

$$f_\perp(s) = \gamma \sin \theta(s) \tag{2}$$

If the contour line curves sharply around a FAS, then we can determine the vertical force $F_\perp$ on a pinning site by integrating $f_\perp(s)$ along the curved section of the contour line that borders the pinning site

$$F_\perp \approx \gamma \int \sin \theta(s)\, ds \tag{3}$$

The accuracy of eq 3 depends on λ. The smaller λ, the closer we can measure the contours around the pinning site and the more accurate eq 3 becomes. The method can be gauged by integrating $\sin \theta(s)$ along the whole contour Γ. The result must equal the total vertical force exerted on the nonadhering part of the vesicle

$$\gamma \int_\Gamma \sin \theta(s)\, ds = F_0 + F \tag{4}$$

with F_0 the vertical force in the absence of the magnetic bead force F. F_0 equals $\gamma_o \int_\Gamma \sin \theta_o(s)\, ds$ with $\tan \theta_o(s)$ the slope of the profile for $F = 0$.

To determine the horizontal (i.e., in-plane) force $F_\parallel$ on a pinning site, we will use a simpler method. In a separate paper,[15] we showed—by generalizing the Joanny−de Gennes theory of wetting on a surface exhibiting pinning holes—that the in-plane force on a pinning site is related to the *apex angle* Φ of the triangular shape of the contact line near the pinning site by

$$F_\parallel = (\kappa\lambda)^{1/2}\theta_c{}^2(\pi/2 - \Phi) \tag{5}$$

with θ_c the contact angle measured away from any pinning sites where we assume that away from pinning sites there is still a well-defined adhesion free energy.

A more fundamental mode of contour force analysis is to determine the height profile directly at the contact line. By minimization of the elastic free energy of a membrane under the boundary condition that both h and $\partial h/\partial n$ vanish at the contact line, it can be shown that the vertical force per unit length on the contact line must equal[9]

$$f_{\perp,c}(s) = \kappa(\partial^3 h/\partial n^3 + \rho_c{}^{-1}(s)\, \partial^2 h/\partial n^2) \tag{6}$$

with s the arclength along the contact line, n the normal to the contact line, $h(n,s)$ the height profile of the vesicle, and $\rho_c{}^{-1}(s)$ the curvature of the contact line. Integrating $f_{\perp,c}(s)$ along the perimeter of a pinning site gives an accurate expression for the force applied by the membrane on the pinning site. The higher order derivatives of the contour can be determined approximately close to the pinning centers and comprise about 30% of the second-order derivatives. However, outside of pinning centers the third-order derivatives can be hardly determined.

It is also possible to obtain the torque per unit length $M(s)$ exerted on the contact line by the nonadhering part of the vesicle from the height profile (cf. also eq 10)

$$M(s) = \kappa \partial^2 h/\partial n^2 \tag{7}$$

A special case is that of a vesicle adhering to a substrate with just a single circular adhesion disk of radius R (cf. Figure 5 below) while a force F is applied in the vertical direction at the opposite pole. The radial height profile $h(r)$ can be determined explicitly (see Appendix A)

$$h(r) = (F/2\pi\gamma)\{\ln(r/R) - (\lambda/R)[K_o(r/\lambda) - K_o(R/\lambda)]K_o'(R/\lambda)\} \tag{8}$$

where K_o is the modified Bessel function (cf. Appendix). If we compute the slope dh/dr we find that, for a large value of r compared to the capillary length λ, the slope $dh/dr \approx (F/2\pi\gamma)\lambda/r$ is inversely proportional to r. This demonstrates explicitly that there is no well-defined contact angle near a pinning site. Using eq 8 in eq 6 gives the (obvious) result

$$f_{\perp,c} = F/2\pi R \tag{9}$$

for the force per unit length on the contact line. The torque per unit length on the contact line is

$$M = (F/2\pi)(\lambda/R)^3[K_o(R/\lambda)/K_o'(R/\lambda)] \tag{10}$$

This important result will be used below.

These methods assume implicitly that unbinding events in the adhesion disk occur at such a low rate that the tension γ of the vesicle surface remains uniform across the nonadhering part of the vesicle, so no currents of lipid are generated along the vesicle surface by tension gradients across the vesicle ("Marangoni currents"). The nonadhering part of the vesicle should be in mechanical equilibrium provided the stress relaxation time τ of the membrane, typically of the order of 5 s, is short compared with the characteristic time scale for the evolution of the adhesion disk. Whether this assumption is valid or not must be answered experimentally on a case-by-case basis.

III. Experiments

(A) High Receptor Coverage. In the first series of experiments, the receptor surface was prepared by incubating the substrate with a 0.017 mg/mL (68 nM) integrin solution. The surface density of the receptors was estimated by total internal reflection fluorescence microscopy by using imunofluorescence techniques (unpublished results). The coverage was 3×10^9 integrins per mm^2, and about 10−20% were active. The receptor-to-RGD ligand ratio was 1:2.8. Figure 2a shows an RICM image of the contact zone before (upper image) and after (lower two frames) application of a force of $F = 1.8$ pN on the magnetic bead. A well-defined adhesion disk is visible. In the center of the disk the membrane is deflected toward the inside forming a blister. This blister does not affect the interpretation of the experiments since the outer perimeter of the blister is well separated from the outer

(15) Albersdoerfer, A.; Bruinsma, R.; Sackmann, E. *Europhys. Lett.* **1998**, *42*, 227−231.

rim of the vesicle. The contact line defining the adhesion disk clearly reveals a set of contact line "pinning centers" (PC) separated by 3−5 μm. As expected theoretically, the contact line near a pinning site has a triangular shape. The apex angle Φ decreases after application of the external force, as can be seen by comparing the first and second frame of Figure 2a. Note that even when the external force is equal to zero, an adhering vesicle still applies a force (F_0 in eq 4) on a pinning center. The difference of the apex angles of the pinning centers (e.g., 1 and 8) in Figure 2a is due to differences of the adhesion strength. Equation 5 is only a rough approximation, which holds for every weak pinning force[15] and which does not account for this fact. In fact the capillary length in eq 5 can be considered as an effective parameter that increases with the adhesion energy of the PCs. This effective value of λ can in principle be estimated from the contour of the PCs (as shown in ref 14) by ignoring that a constant angle cannot be defined as shown in the present paper. For a more detailed study, this aspect would have to be reconsidered more carefully.

To obtain the horizontal force $F_{\parallel}$ exerted on a pinning center by application of eq 5, we divided the height contours into a curved region close to the contact line and a straight region further away (see Figure 2b). The contact angle θ_c was obtained by reconstructing the contour of the vesicle in a direction normal to the contact line in a region of the contact line away from pinning sites (along the white bar in Figure 2a middle). The slope defines the contact angle while the intercept of the asymptotic tangent with the horizontal gives the capillary length λ—and hence γ—according to $\lambda = (\kappa/\gamma)^{1/2}$ (of order 1 μm). After measuring the apex angles, we obtained for the horizontal force $F_{\parallel}$ on pinning sites 1 and 8, respectively, 3.9 and 0.42 fN for an external force $F = 1.2$ pN. When the external force was increased to 1.8 pN, these values increased to 27 and 3.9 fN, respectively. Note that $F_{\parallel}$ depends in a strongly nonlinear way on F.

To obtain the vertical force $f_{\perp}(s)$ per unit length on the contour line, we used eq 3. The result is shown in Figure 2c (for $F = 1.8$ pN), where we plot the force per degree along the angular direction (see Figure 2a, last panel). It follows from Figure 2c that—as expected—$f_{\perp}(s)$ increases sharply near a pinning sites. Integrating the area under these peaks to obtain $F_{\perp}$, we again obtain force values in the 1−10 fN range. For reasonable laboratory time scales, such forces are much too weak to unbind individual ligand−receptor pairs. Since pinning sites may contain a significant number of ligand−receptor pairs, we should not expect that the external force is able to remove pinning sites and, in fact, no unbinding events were observed. Numerical integration, according to eq 4, of the total vertical force yields a value $F_0 + F = 2.1$ pN, in reasonable good agreement with an externally applied force $F = 1.8$ pN. The total horizontal force $F_{\parallel} \approx \gamma \int \sin\theta(s)\, ds$ has been calculated in the absence and presence of the external force by integrating over the whole circumference of the adhesion disk. The resulting in-plane force for a pulling force for $F = 1.8$ pN is of the order of 0.2 pN and is thus zero within experimental error, which provides further evidence for the reliability of our data analysis.

(B) Medium Receptor Coverage. In the next series of experiments, the substrate was incubated with an integrin solution of 0.17 μg/mL (i.e., a factor 100 lower than in the previous case). As shown in Figure 3, the morphology of the adhesion disk is quite different (for $F = 0$): a limited number of tight adhesion spots are visible, denoted by pinning centers (PCs) 1 to 4. In the remainder of the adhesion domains, (gray−white scale), the spacing between the membrane and the substrate is much larger (several 10 nm).

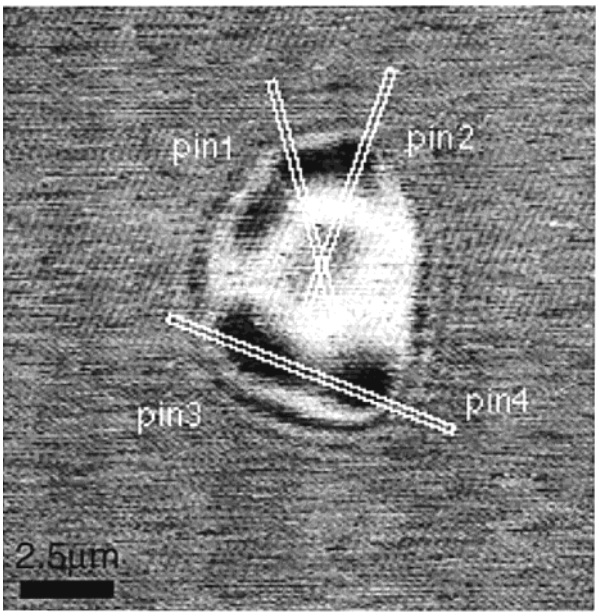

Figure 3. Vesicle adhering to the substrate at four pinning domains (1, 2, 3, 4). The substrate was incubated with 170 ng/mL integrin solution. The white bars mark directions along which time evolution of contours is evaluated in Figure 4.

If we now turn on the magnetic force, we should expect that, since there are only a limited number of pinning sites available, each pinning site is subjected to a larger force than in the previous set of experiments. On the right side of Figure 4, a series of RICM images show the shape changes as a function of time, following force application, along the three sections of the adhesion disk shown in Figure 3. The intensity distributions of the interferograms were recorded every 0.04 s and joined together in such a way that the change of the contour near the substrate is visualized continuously from bottom to top in Figure 4. If the start of the columns is considered to be $t = 0$, then the magnetic force is turned on at $t = 1.2$ s (marked by number 1) to a level of $F = 0.3$ pN. It is increased to $F = 0.6$ pN at $t = 7.2$ s (marked by number 2). The PCs are represented by the dark bands most clearly visible on the left side of the first two columns of Figure 4 (before unbinding). We focus first on PCs 1 and 2. We see first fast vanishing (within 1 s) of one of the fringes (at position 1) after application of the force at $t = 1.2$ s. This is a consequence of the increase of the membrane tension γ (by $F/\pi D$) under the $F = 0.3$ pN force. The tension increases visibly up to 7.2 s since the rim of the contact line moves slightly to the right, when the light gray fringes vanish completely. The time within which the position changes abruptly is a measure for the viscoelastic response time of the vesicle. The diameter of the adhesion disk along the PC 1 scan is equal to the total width of the dark band at the right, and it does not appear to change significantly at $t = 1.2$ s.

Following the increase in force at $t = 7.2$ s, we see that the dark bands of PC1 and 2 vanish after 16.5 and 13 s, respectively (sites marked by number 3). This is due to force-induced unbinding of the pinning center. These unbinding events are clearly seen by inspection of the RICM image of the whole adhesion disk shown on the right side of Figure 4. Note that the unbinding of the pinning center PC 2 occurs at $t = 6.6$ s and that of the PC 1 occurs at $t = 9.4$ s after application of the 0.6 pN force. Note again that the origin of the time scale is arbitrarily

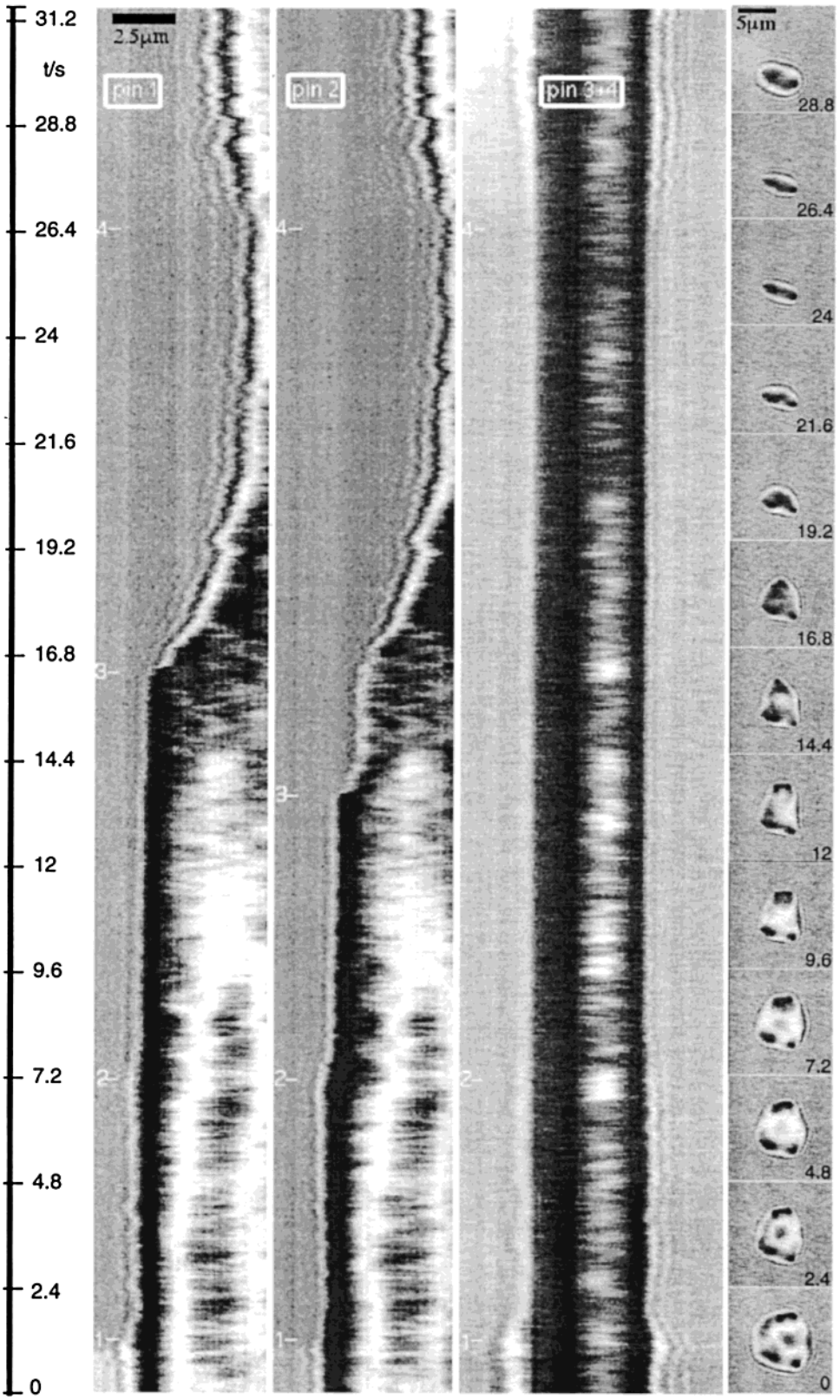

Figure 4. Scenario of partial unbinding of vesicle with four pinning domains (PC 1−4). The left three images show the intensity distribution of the RICM image along sections crossing pinning centers 1−4 (defined in Figure 3). The intensity distribution was measured every 0.04 s and plotted from bottom to top. The time axis in seconds is given at the left. The white numbers 1 and 2 in the middle image mark the time of switching on the force of $f = 0.3$ pN and increasing to $f = 0.6$ pN, respectively. At position 3 pinning centers are ripped off and at position 4 the force of $f = 0.6$ pN is switched off. (Note that the dark bands define the pinning centers, while the diffraction fringes give an impression on the state of tension.) The images on the right column show RICM pictures of the observed vesicle in time intervals of 2.4 s.

fixed at the beginning of the observation and the pulse is applied at time 7.2 s. The adhesion disk diameter along the PC 1 scan decreases, for instance, by an amount of 0.6 μm. The unbinding of the PCs at $t = 6.6$ s and $t = 9.4$ s after application of the force of 0.6 pN suggests that the off-rate of the PC under this force is k_{off} (0.6 pN) $\sim$ 1/7 s

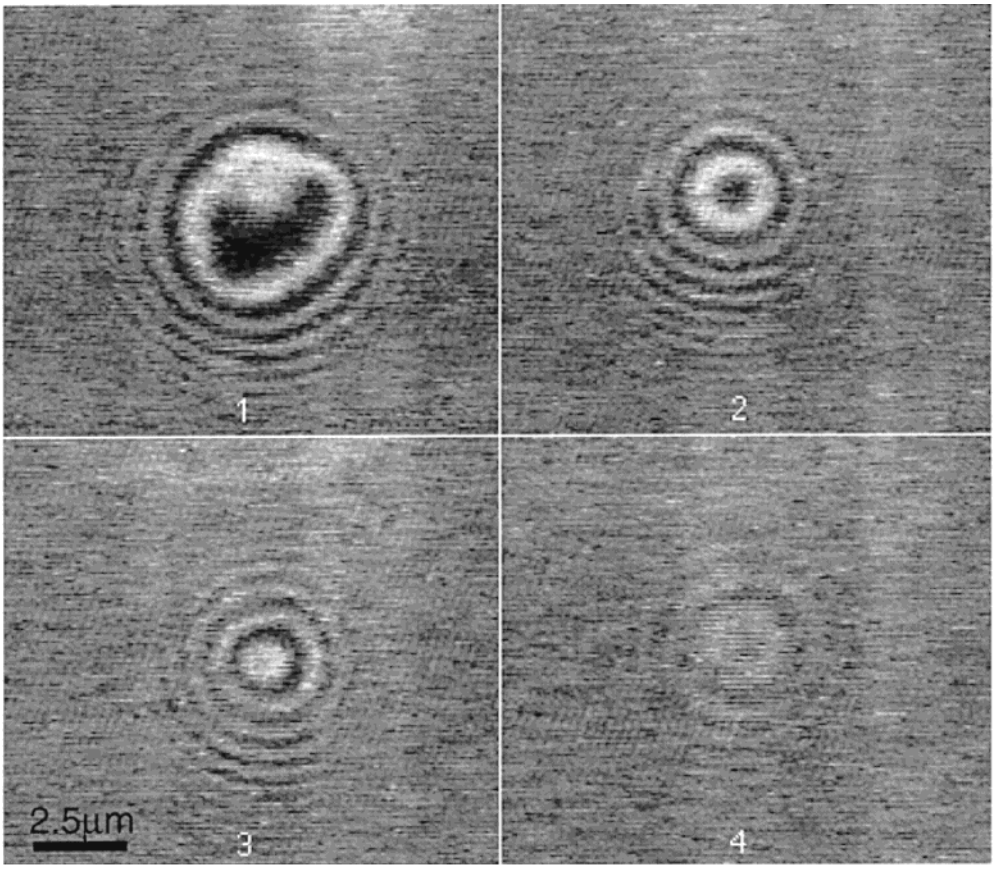

Figure 5. RICM images of a vesicle with a single pinning center adhering to a substrate incubated with 17 ng/mL of integrin. The snapshots for four forces F are shown: $F = 0.15$ pN (1), $F = 0.3$ pN (2), $F = 0.45$ pN (3), and $F = 0.8$ pN (4). For the last force the vesicle was ruptured from the surface and rapidly moved upward.

$\sim$ 0.14 s. The off-rate of the PCs in absence of the force is much longer.

Following the unbinding of the two pinning centers (PC 1 and PC 2), the vesicle relaxes with a time constant τ^{-1} of about 0.30 s, which we identify again with the stress relaxation rate. The remaining two pinning sites do not unbind at the maximum force levels of F that can be reached (about 1 pN). Following stress relaxation after switching off the external force, the tension γ decreases as indicated by the reappearance of the series of fringes. The decay time of γ is again a measure for the relaxation time of the vesicle viscoelastic response.

(C) Low Integrin Coverage. To perform a quantitative analysis on the height profile of single centers, we reduced the integrin coverage further by incubating the substrate with a 17 ng/mL integrin solution with the purpose of finding a vesicle attached with just a single pinning center. As shown in Figure 5, we succeeded in finding such a case. Although for $F = 0$ the adhesion zone is not circular (see panel 1), the adhesion disk becomes (nearly) circular after application of a force of $F = 0.15$ pN (see panel 2) and remains circular as the force is increased up until the unbinding force is reached (see panel 4). The ligand−receptor pairs have apparently been collected into a single patch by the application of the external force even though integrin receptors are immobilized on the surface. Adhesion patches are expected to form at sites of local enrichment of receptors. Moreover the ligands are freely mobile and they can easily accumulate locally by lateral diffusion and repeated dissociation and association.[7] As demonstrated previously[8] the adhesion is a first-order transition driven by competition between short-range attraction and long-range repulsion leading to adhesion induced receptor segregation associated with the formation of metastable adhesion domains.

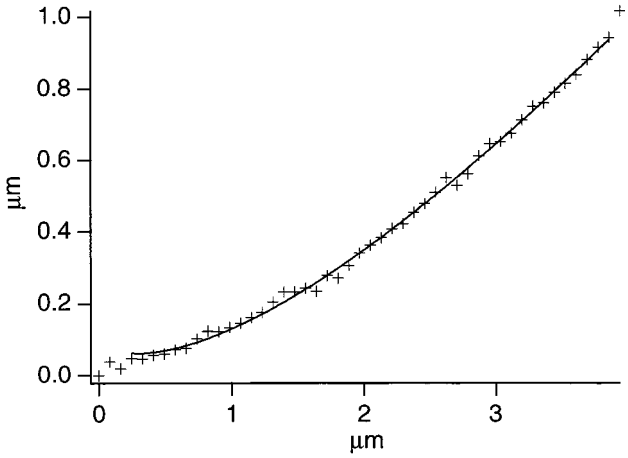

Figure 6. Fitting of eq 8 to contour of vesicle in Figure 5 at $F = 0.3$ pN (image 2).

As discussed in the previous section, the calculation of the height profile simplifies for the case of cylindrical symmetry. We can measure the radial height profile $h(r)$ and fit the result with eq 8 to obtain γ as well as the adhesion-disk radius R. As shown in Figure 6, such a fit produces reasonable results. For an applied force of $F = 0.3$ pN, we obtain in this way a tension γ of 7.4×10^{-9} N/m and a disk radius of about 300 nm while for $F = 0.45$ pN the tension γ increased to 1.5×10^{-8} N/m and R decreased to about 200 nm. For a bending energy of 100 $k_B T$, appropriate for our case, λ is large compared to R. We also confirmed that eq 4 remains valid. The strong dependence

of the tension γ on F indicates that the force-induced tension dominates the adhesion-induced tension, and we can reasonably equate γ with $F/\pi D$.

IV. Discussion

The central result of this study is that, using the magnetic tweezers method, it is possible to unbind pinning centers (or FAS) with applied forces of order of 1 pN or less. Single-molecule force studies of ligand−receptor pairs report rate-dependent unbinding forces in the range of a few piconewtons to 50 pN or more.[2,16] We saw that pinning centers may have a radius of order of 1000 Å. If we assume that the spacing d between adhesion molecules in a tightly packed pinning center is of the order of 100 Å, then a pinning center may contain of the order of 100 paired adhesion molecules. How is it possible that external forces in the range of 1 pN or less can lead to unbinding events? The binding energy of the ligand−receptor pair used in our study is fairly weak but not exceptionally so. Judged from the binding constant of $K_D \approx 1\ \mu$M, one estimates a binding energy of the order $\approx 10\ k_BT$ (unpublished results of this laboratory).

To gain a better insight into this paradox, we consider again the unbinding event of a vesicle having a single circular pinning center of radius R, such as shown in Figure 5. The conditions for mechanical equilibrium of the edge of the adhesion disk are eqs 9 and 10. Equation 9 states that a vertical force per unit length is exerted on the edge of the adhesion disk equal to $F/2\pi R$, with F the external force. Mechanical equilibrium demands that the adhesion molecules along the edge region of the disk apply an equal but opposite force on the membrane. In the case most favorable for unbinding, only the adhesion proteins on the exterior of the adhesion disk are subject to this force per unit length. If ρ_1 is the line density of these proteins, then a protein along the edge must exert a force of order $F/2\pi\rho_1 R$. For ρ_1 of order 1/100 Å, R of order 1000 Å, and F in the piconewton range, this cannot possibly produce any unbinding events, at least for laboratory time scales.

The second condition of mechanical equilibrium requires that the proteins in the border region also must exert a torque per unit length equal to M, as given by eq 10. For small pinning centers with $R \ll \lambda$ (appropriate for Figure 5), eq 10 simplifies to

$$M(R) = (\kappa D/2)(1/R)^2 \ln ((\kappa\pi D/F)^{1/2}/R) \qquad (11)$$

where we equated γ with the force-induced tension $F/\pi D$. Note that M has the dimensions of a *force*. For a vesicle with a diameter D of 30 μm, a bending energy of 100 k_BT, and adhesion disk radius of 1000 Å, this force is of the order of 300 pN. This is a measure for the effective traction force on the domain-like pinning center generated by the moment.

A precise determination of the torque exerted by deformed adhesion proteins at the edge of an adhesion disk requires a microscopic calculation. In Appendix B we provide a simple scaling argument that indicates that the torque-induced force f, which adhesion proteins in the border region must provide, is simply proportional to M

$$f \sim M(\Delta E/\kappa\rho_2 a^2)^{1/2} \qquad (12)$$

with ΔE the characteristic energy of the interaction potential between ligand and receptor, a the characteristic length scale of that potential, and ρ_2 the area density of proteins in the adhesion disk. With ΔE of order 10 k_BT, a of order 1 nm, a bending energy of 100 k_BT, and an area density of order 1/500 Å, f is of order M and hence sufficiently large to generate unbinding events.

Note, from eq 11, that $M(R)$ depends only weakly on the external force F and increases with decreasing R. The second observation indicates that this unbinding scenario has a "run-away" character. Once unbinding starts at the rim, R decreases. According to eq 11, $M(R)$ increases as R decreases and hence, through eq 12, the unbinding force increases.

The mechanism may be illustrated intuitively by considering the height profile $h(r)$ (see eq 11 and Figures 2b and 6). The external force F is not applied directly to the adhesion disk. Because of the stiffness of the membrane, the force is effectively applied at a distance λ from the rim of the adhesion disk. Since λ is large for stiff membranes, the external force is applied via a large *lever arm*. If we assume that the adhesion molecules are fairly rigid and impose a well-defined spacing on the gap between the membrane and the substrate, then adhesion molecules in the rim of the disk only have a small lever arm w (see Appendix B for an estimate of w). As a result, a modest external force can apply a large torque on the edge of the adhesion disk since the applied force is magnified by the mechanical advantage λ/w.

These results appear to provide an interesting insight into the "design aspects" of bioadhesion. Pinning centers, or focal adhesion sites, clearly provide a secure connection between two membranes. Pinning centers contain a large number of adhesion molecules, each having a binding energy of about 10 k_BT, so thermal fluctuations cannot produce any unwanted unbinding events. By application of a steady exterior traction, the leverage effect allows the force to break the connection with force levels that are less than those required to break individual molecular bonds under linear traction. This could explain why in situations requiring strong adhesion the rodlike cell surface receptors are coupled directly to actin stress fibers. Examples are the tethering of endothelial cells to the wall of the blood vessels through integrin $\alpha_v\beta_{III}$ or the formation of tight adhesion plaques between epithelial cells mediated by cadherins.

Concluding Discussion

A new force spectroscopy has been developed enabling force dependence measurements for the unbinding kinetics of membrane bound receptor−ligand pairs under biological relevant conditions. The technique can be applied to study the rupture of single bonds or multiple bonds.[17] Since the unbinding force is applied by pulling the vesicle with a point force in the normal direction, the maximum force rate is determined by the viscoelastic response time of the giant vesicles which is of the order of ∼1 s. The most interesting aspect of the present technique is that it yields detailed insight into the control of adhesion strength by the membrane elasticity and the transmission of the force from the site of attack to the adhesion site by membrane tension and bending moments. The membrane tension can be continuously measured by membrane contour analysis. Theoretical evidence has been provided that due to the lever rule unbinding by moments can be much more efficient than by traction forces. This leverage concept can explain our finding that the bond between integrins and RGD ligands can be broken by pulling forces well below 1 pN at force rates of 1 pN/s. The off-rate at 100 fN is of the order $k_{off} \sim 1/7\ s^{-1}$ ($0.14\ s^{-1}$) compared to $k_{off} \sim$

(16) Florin, E. L.; Moy, V. T.; Gaub, H. E. *Science* **1994**, *264*, 415−417.

(17) Seifert, U. *Phys. Rev. Lett.* **2000**, *84*, 2750−2753.

$0.007\ s^{-1}$ the absence of forces.[11] In the latter study we also showed that strong binding of the cyclic peptide is only possible if it is separated from the vesicle surface by a spacer of 2.4 nm suggesting that this corresponds to the depth of the binding pocket of the integrin. The dissociation constant of the bond is $K_D \sim 10^{-6}$ M, which is orders of magnitude larger than the critical micelle concentration of phospholipids ($\sim 10^{-12}$ M). This rules out the possibility that the unbinding of the vesicles is due to lipid extraction, a process studied by Ludwig and Evans (unpublished results). In this case extraction forces of 2 pN at a force of 1 pN/s were observed.

The finding that receptor−ligand bonds may be much more efficiently broken by leverage rather than by pure traction forces may have important biological consequences. It could explain why cells strengthen the tethering forces by receptor clustering and by coupling to the intracellular domain of receptors to actin stress fibers through focal adhesion complexes. According to eq 11, the torque per unit length decreases with the square of the radius of the adhesion plaque and the strength of the tethering force exerted by a focal adhesion domain increases dramatically with the diameter of the adhesion domain.

Acknowledgment. R.B. thanks the Sonderforschungs Bereich of the TU Muenchen for its support and hospitality as well as NSG Grant DMR-9708646 for financial support. Helpful discussions with Dr. M. Bärmann are gratefully acknowledged. The experimental work was supported by the Fonds der Chemischen Industrie and the Deutsche Forschungsgemeinschaft (SFB 266).

Appendix A

To derive eq 8, we use the free energy of a tensed membrane in the Monge representation

$$H = \frac{1}{2}\int d^2r\{\kappa(\nabla^2 h)^2 + \gamma(\nabla h)^2\} \tag{A1}$$

Minimizing H with respect to h gives

$$\kappa\nabla^4 h - \gamma\nabla^2 h = 0 \tag{A2}$$

For a circular adhesion disk, we must solve eq A2 under the condition that $h(R) = h'(R) = 0$. For a large r value compared to λ, the tension term dominates. In that regime, the integral of the tension along a contour of radius r times the slope $h'(r)$ must equal the external force F, so $\gamma 2\pi r h'(r)$ must be F. Note that $h(r) = C \ln(r)$ is a solution of eq A2, so we must choose $C = F/2\pi\gamma$.

To satisfy the boundary conditions at $r = R$, we must add a second solution of eq A2 which vanishes for large r. It is obvious that any solution of

$$\nabla^2 h - \gamma^{-2} h = 0 \tag{A3}$$

also solves eq A2. In radial coordinates, eq A3 is solved by the modified Bessel functions. Requiring cylindrical symmetry and demanding that the solution vanishes for large r only leaves $K_0(r/\lambda)$ as an appropriate solution. Hence, looking for a general solution of the form

$$h(r) = (F/2\pi\gamma)\ln(r) + cK_0(r/\lambda) + d \tag{A4}$$

we can fit the boundary conditions with the result given in the text (Figure 7).

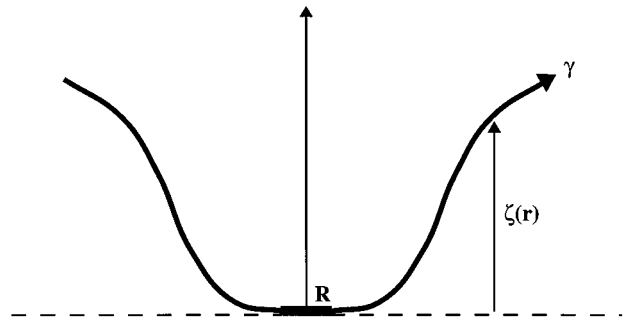

Figure 7.

Appendix B

To derive eq 12, we assume a disk of packed adhesion molecules exhibiting an area density ρ_2 (a pinning center or FAS). The external torque per unit length M stretches the ligand receptor bonds in a rim running along the edge of the adhesion disk. Let w be the width of rim and let f be the force exerted on individual ligand−receptor pairs in the rim. The torque generated by one pair is then of order of fw. The torque per unit length produced by the adhesion molecules is then $\rho_2 f w^2$ since the rim has a width w. According to the lever rule of Archimedes, the torque per unit length produced by the adhesion molecules must be equal and opposite to the externally applied torque M per unit length

$$M \sim \rho_2 f w^2 \tag{B1}$$

Next, let R_c be the radius of curvature of the membrane at the contact line, so $M \sim \kappa/R_c$. Let δh be the typical distance an adhesion molecule of the rim is stretched along the vertical direction. If $v(h)$ is the ligand−receptor interaction potential, then we estimate

$$f \sim v''(0)\,\delta h \tag{B2}$$

It should be noted that the interaction potential depends on the elastic deformation of the membrane and the ligand as well as on the chemical potential of the receptors and the repellers in the free membrane area.[8] We now demand that the characteristic curvature of the rim area, $\delta h/w^2$, equals that of the membrane ($1/R_c$) so

$$f \sim v''(0) w^2/R_c \tag{B3}$$

Eliminating w from eq B1 gives

$$M \sim \rho_2 f^{\,2} R_c/v''(0) \tag{B4}$$

Finally, using $M \sim \kappa/R_c$ to eliminate R_c, we obtain the desired relation between the applied moment M and the stretching force f which boundary proteins are subjected to

$$f \sim M(v''(0)/\kappa\rho_2)^{1/2} \tag{B5}$$

LA000279X